Angle-differential Stokes parameters for spin-polarized electron-impact excitation of the Hg $6s6p\ ^3P_1$ state at 25-eV scattering energy

F. Jüttemann and G. F. Hanne
Physikalisches Institut, Universität Münster, Wilhelm-Klemm-Straße 10, D-48149 Münster, Germany

O. Zatsarinny and K. Bartschat
Department of Physics and Astronomy, Drake University, Des Moines, Iowa 50311, USA

R. Srivastava and R. K. Gangwar
Department of Physics, Indian Institute of Technology, Roorkee, India

A. D. Stauffer
Department of Physics and Astronomy, York University, Toronto, M3J 1P3, Canada
(Received 24 September 2009; published 21 January 2010)

Results of spin-resolved angle-differential Stokes parameters from electron-photon coincidence studies of electron-impact excitation of the $6s6p\ ^3P_1$ state of mercury, resulting in 254 nm radiation, are presented. Due to the intermediate-coupling nature of the excited state, the wave function of this state has a small singlet part. With increasing scattering energy, the influence of exchange scattering decreases, so that direct scattering via the singlet part can become relevant. Recent angle-integrated Stokes-parameter measurements indicated that exchange is still important for the 254 nm line ($6s6p\ ^3P_1 \rightarrow 6s^2\ ^1S_0$) up to at least 50 eV incident energy [Jüttemann *et al.*, Phys. Rev. A **79**, 042712 (2009)]. At energies above 15 eV, however, cascade effects complicate a detailed comparison of these angle-integrated results with theoretical calculations. The angle-differential Stokes parameters presented here are unaffected by cascade effects due to the coincidence technique and thus allow for an analysis of the discrepancies observed by Jüttemann *et al.* and also by Srivastava *et al.* [Phys. Rev. A **80**, 022718 (2009)]. Comparison of the experimental data with theoretical predictions reveals that the description of the initial target state and the excited state in intermediate coupling have a significant influence on the overall agreement.

DOI: 10.1103/PhysRevA.81.012705 PACS number(s): 34.80.Dp

I. INTRODUCTION

For electron scattering from heavy target atoms, such as Hg with nuclear charge $Z = 80$, significant spin effects are generally expected due to electron exchange and the spin-orbit interaction both in the target alone and in the electron-target interaction. These scattering mechanisms can be studied on the most fundamental level by performing spin-resolved electron-atom collision experiments [1,2].

The particular interest of the present work lies in the intermediate-coupling nature of the Hg $6s6p$ excited states with total electronic angular momentum $J = 1$. These states are usually labeled as "$6s6p\ ^3P_1$" and "$6s6p\ ^1P_1$," respectively, thus giving only the dominant configuration and the coupled spin of the two valence electrons. In the intermediate-coupling description, the wave function of the "$6s6p\ ^3P_1$" state has a small singlet component. The contribution of this part of the wave function to the excitation is expected to become more and more significant with increasing scattering energy because the dominant excitation mechanism for the triplet part is via exchange, which diminishes with increasing energy. Recent angle-integrated Stokes-parameter (light-polarization) measurements for the $6s6p\ ^3P_1 \rightarrow 6s^2\ ^1S_0$ transition (254 nm) [3] showed, as expected, decreasing exchange effects with increasing scattering energies from 15 to 50 eV. The comparison of these experimental data with predictions from a 36-state fully relativistic Dirac B-spline R-matrix (DBSR-36) close-coupling-type calculation revealed qualitative agreement, but the calculation predicts considerably stronger exchange effects than observed experimentally. The comparison of recent relativistic distorted-wave (RDWBA) results [4] with the experimental data from Ref. [3] exhibited similar discrepancies. However, these differences between experiment and theory can be largely caused by cascading from higher levels excited by electron-impact.

The principal motivation for the present work, therefore, was the investigation of exchange and direct effects without significant influence of cascades to further analyze the discrepancies mentioned previously. Specifically, angle-differential Stokes parameters for the $6s6p\ ^3P_1 \rightarrow 6s^2\ ^1S_0$ transition were measured in an electron-photon coincidence experiment at a scattering energy of 25 eV. By setting a time window to correlate the excitation process and the photon emission, cascade contributions can effectively be eliminated from the observed signal.

This article is organized as follows. After discussing some general features of the experiment in Sec. II, we present a brief summary of the experimental method (Sec. III). Following an outline of the numerical approaches (Sec. IV), we present and discuss our results in Sec. V.

II. GENERAL CONSIDERATIONS

A. Scattering geometry and observables

The excited state is studied by analyzing the polarization of the emitted light in coincidence with the scattered electron. The polarization vector $\boldsymbol{P}$ of the incident electrons is chosen

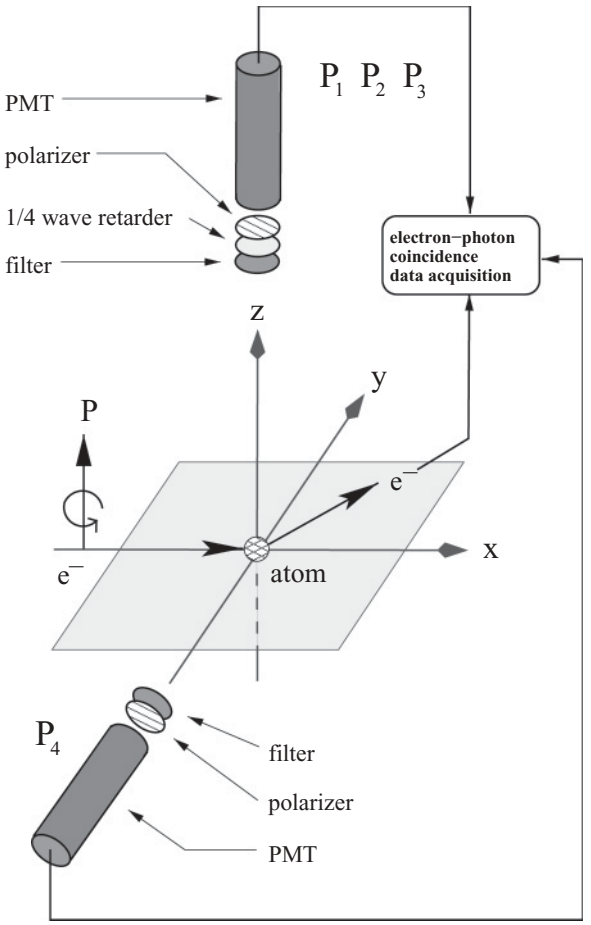

FIG. 1. Schematic illustration of the experimental setup. The coordinate system shown is the *natural frame*, in which the incident beam axis defines the x direction and the quantization (z) axis is chosen as the normal vector to the collision plane.

to be perpendicular to the scattering plane. The photons are observed perpendicular to the scattering plane (along the z direction of the *natural frame*) as well as in the scattering plane (along the negative y direction) as indicated in Fig. 1.

The physical importance of angle-differential Stokes parameters was discussed in detail by Andersen *et al.* [5]. For light observation along the z and the negative y axes of the *natural frame* (see Fig. 1) the Stokes parameters are defined by

$$P_1 = \frac{I_z(0^\circ) - I_z(90^\circ)}{I_z(0^\circ) + I_z(90^\circ)}, \tag{1}$$

$$P_2 = \frac{I_z(45^\circ) - I_z(135^\circ)}{I_z(45^\circ) + I_z(135^\circ)}, \tag{2}$$

$$P_3 = \frac{I_z(\sigma^-) - I_z(\sigma^+)}{I_z(\sigma^-) + I_z(\sigma^+)}, \tag{3}$$

$$P_4 = \frac{I_{-y}(0^\circ) - I_{-y}(90^\circ)}{I_{-y}(0^\circ) + I_{-y}(90^\circ)}. \tag{4}$$

Here $I_{z,-y}(\alpha)$ denotes the light intensity (observed along the z and $-y$ directions), which is transmitted by a linear polarizer aligned at an angle α with respect to the direction of the incident electron beam (x axis), while $I(\sigma^+)$ and $I(\sigma^-)$ are the transmitted intensities of circularly polarized light with positive and negative helicity, respectively.

B. Excitation process

The wave functions of the Hg $6s6p$ ($J = 1$) excited states are often described in the intermediate coupling scheme (see, e.g., Ref. [6]) as

$$\Psi(6^3P_1) = \alpha\Psi^0(6^3P_1) + \beta\Psi^0(6^1P_1), \tag{5}$$

$$\Psi(6^1P_1) = \alpha\Psi^0(6^1P_1) - \beta\Psi^0(6^3P_1). \tag{6}$$

Here Ψ^0 denotes a pure LS-coupled wave function, with $\alpha = -0.987$ and $\beta = 0.171$ [7] representing the mixing coefficients. Note that $\alpha^2 + \beta^2 = 1$.

Equation (5) shows that the wave function of the $6s6p\ ^3P_1$ state has a singlet component. This part of the wave function contributes to excitation via direct scattering. The characteristics of direct and exchange scattering for increasing incident energy were discussed in detail by Jüttemann *et al.* [3]. Their basic argument was that the cross sections for excitation of spin and optically allowed transitions (e.g., excitation of a $^1P_1$ state from a $^1S_0$ state) usually show a slow increase from the excitation threshold and reach a maximum at intermediate scattering energies. In contrast to that, excitation cross sections for spin-forbidden transitions (such as the excitation of a pure $^3P_1$ state from a $^1S_0$ state) show a peak close to the excitation threshold and rapidly fall off with increasing scattering energy. Thus, at energies close to the excitation threshold, a strong influence of excitation via the triplet part is expected for the $6s6p\ ^3P_1 \rightarrow 6s^2\ ^1S_0$ optical transition since it represents the main part in that wave function. With increasing energy, however, its influence is expected to decrease relative to excitation via the small singlet part, due to the general energy dependence of the cross sections for optically allowed and forbidden transitions. As a result, the small singlet part of the wave function will ultimately dominate the excitation of the $6s6p\ ^3P_1$ state.

C. Hyperfine depolarization

The present experiment was performed on the natural isotope mixture of Hg, which contains nuclear spins of $I = 0$ (69.95%), $I = \frac{1}{2}$ (16.87%), and $I = \frac{3}{2}$ (13.18%) [8]. Since the hyperfine structure is not resolved experimentally, the measurement process averages over a mixture of nuclear spins I, which leads to a depolarization of the observed radiation. Consequently, appropriate perturbation coefficients must be used (for details, see Ref. [9]) to account for this effect in numerical calculations. This is done in the present work.

III. EXPERIMENT

The experimental procedure used in the present work is similar to that of earlier studies, for which a detailed description of the experimental setup was given by Herting *et al.* [10]. Briefly, a spin-polarized electron beam (140 meV FWHM energy width) is extracted from a GaAs photocathode and focused onto a beam of Hg atoms from an oven. Photons emitted during the decay of excited Hg atoms from the $6s6p\ ^3P_1$ state into the $6s^2\ ^1S_0$ ground state are selected by an

interference filter, analyzed with a polarization filter system, and finally detected by a photomultiplier. Special care was taken to determine the analyzing power of the polarization filter for the corresponding wavelength of 254 nm and to avoid depolarization due to radiation trapping.

In contrast to earlier studies, a multichannel electron analyzer [11] was used in the current experimental setup to detect scattered electrons with the designated energy loss of 4.89 eV (excitation energy of the $6s6p\ ^3P_1$ state [12]). The use of the multichannel electron analyzer allows us to detect, simultaneously, electrons that are scattered through eight different angles with an angular separation of 14°. The measurement process for each Stokes parameter consists of two sequences. Between sequences the multichannel electron analyzer was rotated by 7°. In doing so, the experimental data for each Stokes parameter is available in 7° steps. Because of the simultaneous data acquisition for different scattering angles in each sequence, the overall data acquisition time for a coincidence experiment is reduced significantly.

The polarization $|\boldsymbol{P}| = 0.28$ of the incident electron beam was measured at regular intervals using a high-energy (120 keV) Mott detector. Positive and negative electron polarizations can be achieved by simply switching the voltage of a Pockels cell in the laser beam for the photocathode irradiation. From the observed coincidences between photons and electrons, spin-resolved Stokes parameters renormalized to a 100% incident-electron spin polarization can be determined using the procedure described by Herting *et al.* [10]. Spin-averaged Stokes parameters can be calculated by adding the coincidence counts measured with positive and negative electron polarizations. Note that adding these counts doubles the actual data acquisition time. Thus, in situations where the coincidence count rates are very low (e.g., large scattering angles), at least spin-averaged Stokes parameters can be evaluated.

IV. COMPUTATIONAL MODELS

The details of the RDWBA calculations are given in Ref. [4]. Two calculations were carried out that differed in the wave functions used to represent the ground and excited states. The spectroscopic-configuration ground-state (SCGS) wave functions include the minimal configurations necessary to describe these two states while the multiconfiguration ground-state (MCGS) wave functions contain additional configurations of the same total angular momentum and parity. The list of configurations included and their contributions to the total wave function are given in our previous article [4].

The DBSR calculations were described in detail by Zatsarinny and Bartschat [13]. The 36-state model denoted as DBSR-36 closely coupled the states that can be formed from the principal configurations $6s^2$, $6p^2$, $6s7s$, $6s7p$, and $6s6d$, as well as a number of autoionizing states with configurations $5d^96s^26p$ and $5d^96s^27s$. For the present work, we even extend the model by adding another 54 discrete and autoionizing states. We will see that the results of the DBSR-36 and DBSR-90 models are very similar, thereby indicating that the DBSR results are essentially converged with the number of discrete states included in the close-coupling expansion.

It is certainly possible that coupling to the target continuum will change the results to some extent. Unfortunately, we are not yet in a position to perform converged R-matrix with pseudo-states (RMPS) calculations with the DBSR code. However, another aspect of the calculation is the quality of the target description. Overall, the DBSR model gives an excellent *ab initio* description of the energy levels (see Table I of Ref. [13]). The oscillator strength for the $6s^2\ ^1S_0 \rightarrow 6s6p\ ^1P_1$ transition (1.15) is also in very good agreement with experiment (1.16), whereas the theoretical value of 0.016 for the $6s^2\ ^1S_0 \rightarrow 6s6p\ ^3P_1$ transition is significantly smaller than the 0.024 found experimentally (see Table II of Ref. [13] and references therein). In the simple intermediate-coupling picture, this means that the singlet admixture to the $6s6p\ ^3P_1$ is too small in the DBSR models. Since the present experiment is designed to probe exactly this admixture, one may expect problems despite the overall very good target description.

The corresponding oscillator strengths for the structure models used in the RDWBA calculations were 0.0477 (2.53) for the $^3P_1$ ($^1P_1$) final states in the SCGS model and 0.0216 (2.663) for MCGS. Although the absolute numbers in the SCGS model are larger than the experiment by about a factor of 2 due to the neglect of core-valence correlation, the ratio of the oscillator strengths in the SCGS model (0.0189) is closest to the experiment (0.0207). Hence, the improvement in the absolute value of the oscillator strength for the $^3P_1$ final state in the MCGS model comes with the price of a much less accurate ratio and, therefore, most likely an inaccurate account of the singlet-triplet mixing in the two states.

V. RESULTS AND DISCUSSION

Before we discuss the results in detail, we emphasize that the measured P_4 data for small scattering angles (<15°) may be considerably less than the actual value due to an averaging process over the solid angle of the electron spectrometer. This was discussed in detail by Simon *et al.* [14].

A. P_1, P_2, P_3, and P_4

Figures 2 and 3 show the results for P_1, P_2, P_3, and P_4 for a scattering energy of 25 eV. The experimental data are compared with DBSR and RDWBA predictions. For both theoretical approaches there are two sets of results available, which differ in the complexity of the target description (in RDWBA) and the number of coupled states (in DBSR).

In general, all theoretical calculations achieve at least a qualitative agreement with the measurements, reproducing the basic structure of the experimental data as well as the differences between spin-resolved and spin-averaged results. Beyond that, adding more discrete and autoionizing states in the DBSR close-coupling expansion hardly affects the predictions, while changing the complexity of the target description in the RDWBA calculation changes the results considerably. Further general remarks can be made regarding the spin-dependence of the Stokes parameters. The experimental data as well as the theories exhibit substantial spin effects for scattering angles as small as 18°. These spin effects

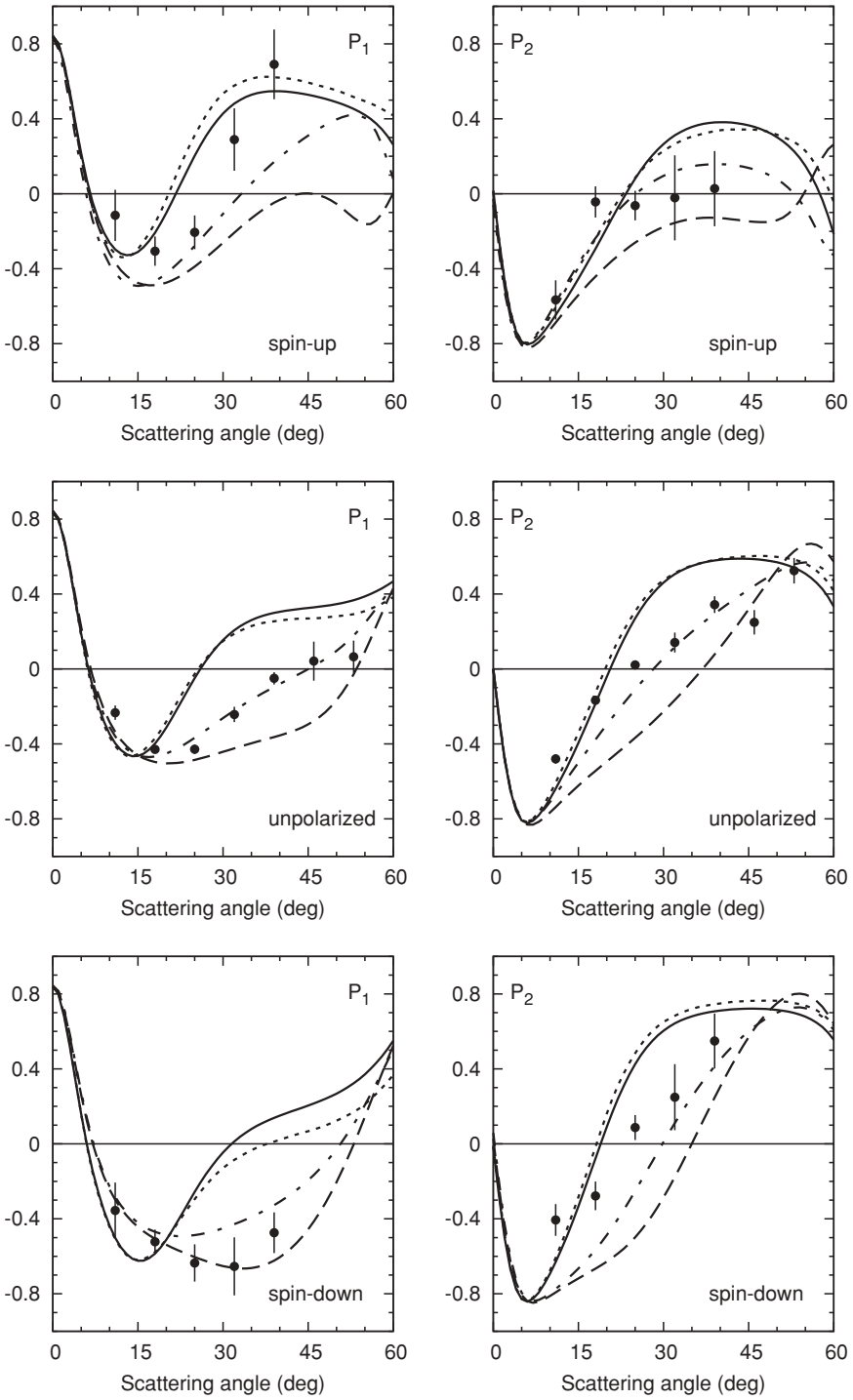

FIG. 2. Stokes parameters P_1 and P_2 for the 254 nm line ($6s6p\ ^3P_1 \rightarrow 6s^2\ ^1S_0$) at 25-eV scattering energy. Experimental data (•) and theoretical calculations: DBSR-36 (· · · ·), DBSR-90 (——), and RDWBA with SCGS (– · – ·) and MCGS (– – – –).

typically result from the resolved fine-structure in combination with electron exchange [15] rather than from Mott scattering, which usually manifests itself at larger scattering angles.

Moving on to the individual Stokes parameters, we note that both the DBSR calculations and the RDWBA with the MCGS are only in qualitative agreement with the experimental data for P_1 at scattering angles larger than 15°. Employing the SCGS in the RDWBA calculation, on the other hand, yields good agreement with the experimental P_1 data, except for spin-up electrons at larger scattering angles.

For the Stokes parameter P_2 the situation is similar in that the SCGS in the RDWBA model again yields the best overall agreement with the experimental data. The DBSR calculations in this case also achieve good agreement for scattering angles smaller than 20°, but the results are too high for larger angles. Using the MCGS in the RDWBA calculations again achieves only qualitative agreement with the measurements.

In the case of P_3, the MCGS in the RDWBA calculations shows the best overall agreement, although the predictions for spin-down electrons are significantly higher than the

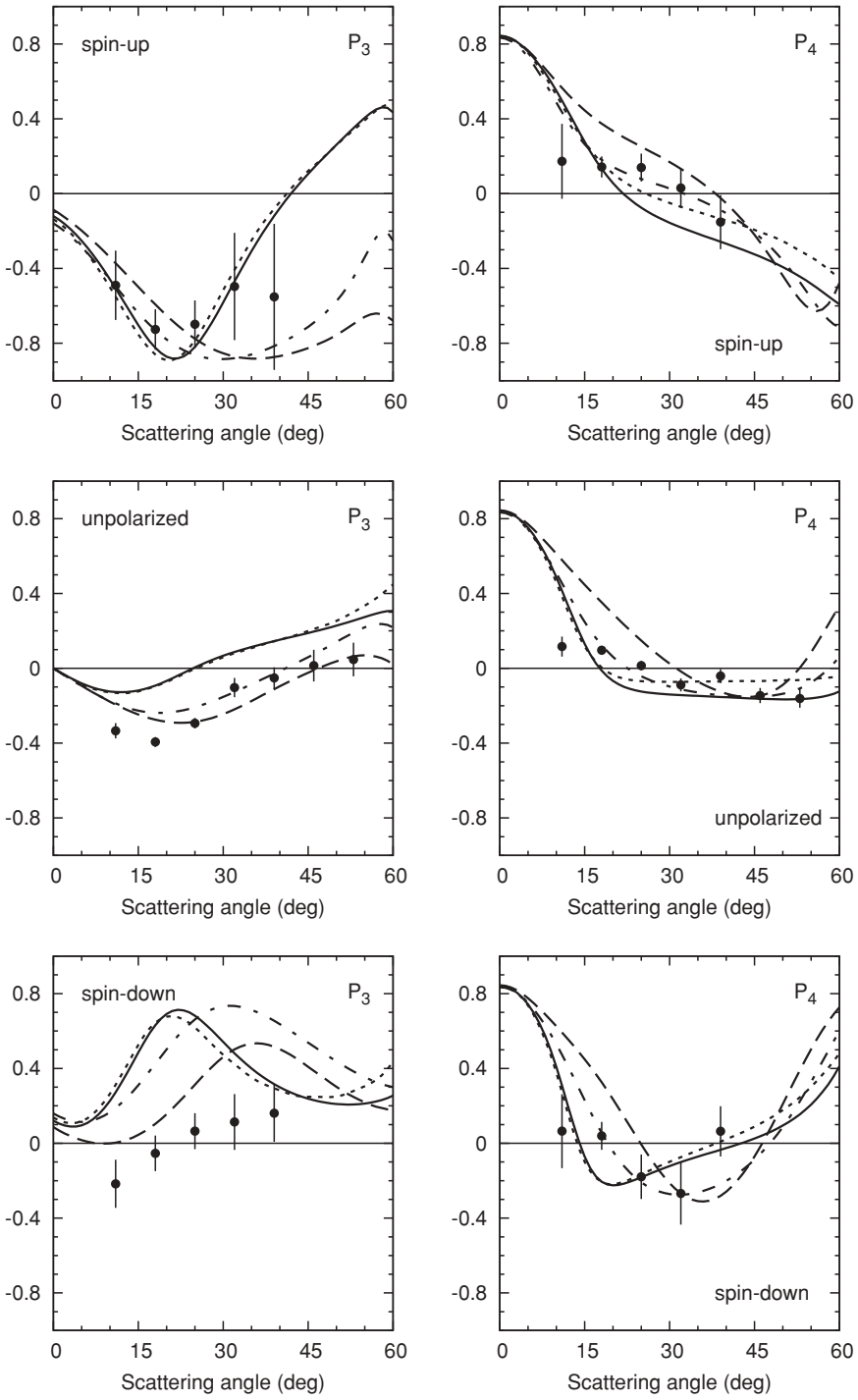

FIG. 3. Stokes parameters P_3 and P_4 for the 254 nm line ($6s6p\ ^3P_1 \rightarrow 6s^2\ ^1S_0$) at 25-eV scattering energy. Experimental data and theoretical calculations as in Fig. 2.

experimental data. The SCGS produces very similar results, but predicts even higher values for spin-down electrons, so that the overall agreement is not as good. The DBSR calculations are in qualitative agreement with the experimental data, but the results for unpolarized and spin-down electrons are too high.

Finally, all theoretical calculations are in reasonably good agreement with the experimental data for the Stokes parameter P_4, with the SCGS of the RDWBA calculation once again showing the best overall agreement. Note that the measured P_4 data point at an 11° scattering angle is almost certainly significantly smaller than the actual value due to an averaging process over the solid angle of the electron spectrometer [14].

B. P_{total}

Figure 4 exhibits the results for P_{total} calculated from P_1, P_2, and P_3 for excitation with unpolarized electrons. The experimental data are compared with DBSR and RDWBA calculations as in Figs. 2 and 3. As expected from the results for the individual parameters, the RDWBA results obtained with the SCGS are in best overall agreement with the measurements.

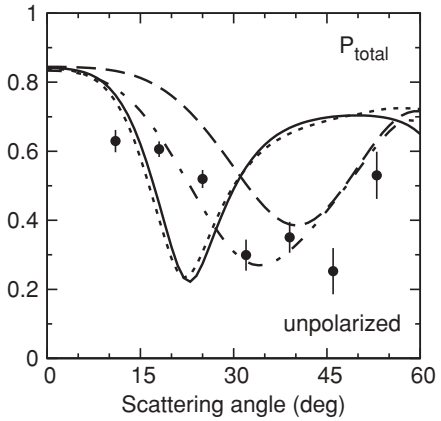

FIG. 4. Total polarization P_{total} for the 254 nm line ($6s6p\ ^3P_1 \rightarrow 6s^2\ ^1S_0$) at 25-eV scattering energy. Experimental data and theoretical calculations as in Fig. 2.

VI. SUMMARY AND CONCLUSIONS

We present experimental and theoretical results for spin-resolved light polarization measured in an electron-photon coincidence experiment for electron-impact excitation of the $6s6p\ ^3P_1$ state in Hg. The coincidence setup was chosen to eliminate, as much as possible, the effects of cascades and the incident energy of 25 eV was chosen to sensitively probe the energy-dependent effect of the singlet admixture to the excited state in the collision process.

The experimental results are compared with predictions from two fully relativistic theoretical models, a distorted-wave (RDWBA) and a B-spline R-matrix (DBSR) approach. Somewhat surprisingly, the least sophisticated theoretical model, namely the RDWBA with a minimal-configuration expansion in the target description, gave the overall best agreement with the measurements. We believe that the reason for this outcome is the fact that this particular target description, fortuitously, gave the best *ratio* of oscillator strengths for the excitation of the two $(6s6p)\ J = 1$ states. Although the absolute values of these oscillator strengths are significantly too large, the ratio effectively determines the outcome of the present calculations.

This is another example of the difficulty faced by state-of-the-art theories in describing the outcome of collision experiments for complex heavy targets such as Hg. In contrast to structure calculations, the variational principle can generally not be used to ensure that improving a collision model, by using a better target description and/or by adding more states to the close-coupling expansion, will lead to improved agreement with the experiment. Clearly, a "perfect theory" not only needs to be able to reproduce relative parameters accurately, but also the absolute value of the respective cross sections and oscillator strengths.

ACKNOWLEDGMENTS

This work was supported, in part, by the Deutsche Forschungsgemeinschaft (F.J. and G.F.H.) and by the US National Science Foundation under Grant Nos. PHY-0757755 and PHY-0903818 (O.Z. and K.B.). A.D.S. wishes to thank NSERC Canada for financial support for this work. R.S. and R.K.G. are thankful to the Council of Scientific and Industrial Research (CSIR), New Delhi, for financial support.

[1] J. Kessler, *Polarized Electrons*, 2nd ed. (Springer-Verlag, New York, 1985).
[2] N. Andersen and K. Bartschat, *Polarization, Alignment, and Orientation in Atomic Collisions* (Springer-Verlag, New York, 2001).
[3] F. Jüttemann, G. F. Hanne, O. Zatsarinny, and K. Bartschat, Phys. Rev. A **79**, 042712 (2009).
[4] R. Srivastava, R. K. Gangwar, and A. D. Stauffer, Phys. Rev. A **80**, 022718 (2009).
[5] N. Andersen, K. Bartschat, J. T. Broad, and I. V. Hertel, Phys. Rep. **279**, 251 (1997).
[6] J. C. McConnell and B. L. Moiseiwitsch, J. Phys. B **1**, 406 (1968).
[7] A. Lurio, Phys. Rev. **140**, A1505 (1965).
[8] P. De Bievre and P. D. P. Taylor, Int. J. Mass Spectrom. Ion Phys. **123**, 149 (1993).
[9] A. Wolcke, K. Bartschat, K. Blum, H. Borgmann, G. F. Hanne, and J. Kessler, J. Phys. B **16**, 639 (1983).
[10] C. Herting, G. F. Hanne, K. Bartschat, A. N. Grum-Grzhimailo, K. Muktava, R. Srivastava, and A. D. Stauffer, J. Phys. B **35**, 4439 (2002).
[11] C. Herting, F. Jüttemann, Z. Petuker, S. Schmitter, and G. F. Hanne, Rev. Sci. Instrum. **79**, 023304 (2008).
[12] Y. Ralchenko, A. E. Kramida, J. Reader, and NIST ASD Team, NIST Atomic Spectra Database (version 3.1.4) (2008), http://physics.nist.gov/asd3.
[13] O. Zatsarinny and K. Bartschat, Phys. Rev. A **79**, 042713 (2009).
[14] T. Simon, M. Sohn, G. F. Hanne, and K. Bartschat, J. Phys. B **23**, L259 (1990).
[15] G. F. Hanne, Phys. Rep. **95**, 95 (1983).